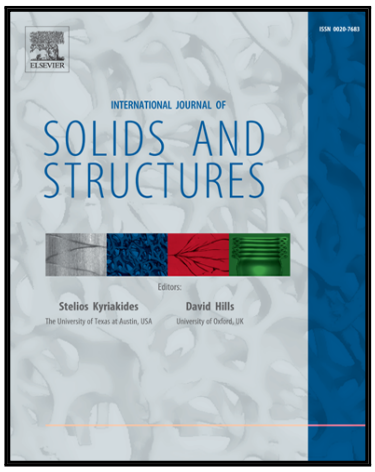

EFFECT OF CYLINDRICAL FIBERS, WITH CROSS-SECTIONS FORMED BY TWO CIRCULAR ARCS, ON THE OVERALL CONDUCTIVITY OF A COMPOSITE.

L. Lanzoni , E. Radi , I. Sevostianov

PII: S0020-7683(18)30020-9
DOI: 10.1016/j.ijsolstr.2018.01.018
Reference: SAS 9867

To appear in: *International Journal of Solids and Structures*

Received date: 29 August 2017
Revised date: 8 January 2018
Accepted date: 11 January 2018

Please cite this article as: L. Lanzoni , E. Radi , I. Sevostianov , EFFECT OF CYLINDRICAL FIBERS, WITH CROSS-SECTIONS FORMED BY TWO CIRCULAR ARCS, ON THE OVERALL CONDUCTIVITY OF A COMPOSITE., *International Journal of Solids and Structures* (2018), doi: 10.1016/j.ijsolstr.2018.01.018

EFFECT OF CYLINDRICAL FIBERS, WITH CROSS-SECTIONS FORMED BY TWO CIRCULAR ARCS, ON THE OVERALL CONDUCTIVITY OF A COMPOSITE.

L. Lanzoni[1], E. Radi[2], I. Sevostianov*[3, 4]

[1] *Dipartimento di Ingegneria "Enzo Ferrari", Università di Modena e Reggio Emilia, Via Vivarelli, 10- 41125 Modena, Italy.*

[2] *Dipartimento di Scienze e Metodi dell'Ingegneria, Università di Modena e Reggio Emilia, Via Amendola, 2 - 42122 Reggio Emilia, Italy.*

[3] *Department of Mechanical and Aerospace Engineering, New Mexico State University, Las Cruces, NM 88001, USA.*

[4] *Center for Design, Manufacturing, and Materials, Skolkovo Institute of Science and Technology, Skolkovo, Russia*

* Author for correspondence: igor@nmsu.edu

Abstract.

An analytic solution for the steady-state temperature distribution in an infinite conductive medium, containing non-conductive fiber with the cross-section of irregular shape formed by two circles, and subjected to remotely applied uniform heat flux is obtained. The temperature flux on the surface of the inhomogeneity is then determined as a function of the geometrical parameters. This result is used to calculate resistivity contribution tensor for the fiber and to evaluate effective conductive properties of a material containing multiple inhomogeneities of this shape.

Keywords

Fiber reinforced composite; irregular cross-section; bipolar coordinates; temperature field; effective conductivity.

1. Introduction.

In this paper, we discuss materials containing a non-conductive cylindrical inhomogeneity with a cross-section formed by two circles. We distinguish between four different shapes of the cross-section presented in Figure 1: (a) two separate circles (auxiliary problem), (b) cross-section formed by union of two overlapping circles of generally different radii, (c) lenticular cross-section (that is mathematically a particular case of two overlapping circles), and (d) lunar cross-section (including arc crack as a limiting case). Such inhomogeneities occur in both natural and man-made materials. Figure 2 provides several examples: (a) electrospinned polystyrene fiber (from Liu et al, 2015) (b) oxidized polyacrylonitrile fiber (from Marcuzzo et al, 2013) (c) natural sisal fiber (Monteiro et al,

2011).

It is well known (see, for example, Torquato, 2002) that the overall conductivity in the direction along the fibers is given by the arithmetic averages of the phases since the electric field in the longitudinal direction is the same constant in each phase. The overall conductivity in the plane normal to the fibers depends on the shape of the cross-sections and fibers arrangement. Analytical modeling of materials with fibers of non-elliptical cross-section is not well developed though many two-dimensional problems have been solved for inhomogeneities of irregular shape (especially in the context of elastic properties). The main approaches to this problem are:

¶ Complex variables technique involving conformal mapping of the considered shape onto a unit circle. For many non-elliptical shapes, the transformation

$$z(\zeta) = R\left(\frac{1}{\zeta} + \sum_{n=1}^{N} a_n \zeta^n\right) \tag{1.1}$$

that maps conformally the exterior of the hole in the complex z-plane into the interior of a unit circle in the ζ-plane, is used, with different parameters R, N and a_n corresponding to holes of various shapes; for the elliptical hole, for example, $N=1$, $R=(a+b)/2$ and $a_1=(a-b)/(a+b)$. For ñirregularò shapes, a numerical mapping technique can be used; note that Tsukrov and Novak (2004) proposed a modification that improves its efficiency;

¶ Finite element method, that is more universal, applies to inhomogeneities of arbitrary elastic properties, including anisotropic ones, but has lower accuracy than the numerical conformal mapping technique. Comparison of the two methods was given by Tsukrov and Novak (2002).

As far as *compressibility* of non-elliptical holes is concerned, it was first analyzed by Zimmerman (1986) on the example of square-type holes (convex and concave), by Givoli and Elishakoff (1992) and Ekneligoda and Zimmerman (2008a) who considered holes with ñcorrugatedò boundaries and by Ekneligoda and Zimmerman (2006, 2008b) who considered shapes having *n*-fold symmetry axes. Results for the entire compliance contribution tensor of a non-elliptical hole have been obtained by Kachanov et al (1994) and Jasiuk (1995) for various polygons (convex and concave) and Tsukrov and Novak (2002, 2004) for several ñirregularò shapes.

In the present paper, we focus on the shapes that may be obtained by union or intersection of two circles of generally different diameters (Figure 1). The shapes may be non-convex and even not simply connected. Application of the conformal mapping technique in this case seems to be a problem. Instead we develop an analytic approach based on Fourier series representation or Fourier transform (dependent on the specific geometry) in bipolar cylindrical coordinates. We consider

thermally conductive plane containing two non-conductive circular inhomogeneities of radii r_1 and r_2 (that may overlap). Following Jeffery (1921), we use bipolar coordinate system (a, b) (Figure 3) related to the Cartesian coordinates (x_1, x_2) by

$$a = \mathrm{Re}\left[\ln \frac{(x_1 + ix_2) + a}{(x_1 + ix_2) - a}\right]; \qquad b = -\,\mathrm{Im}\left[\ln \frac{(x_1 + ix_2) + a}{(x_1 + ix_2) - a}\right] \tag{1.2}$$

$$x_1 = \frac{a \sinh a}{\cosh a - \cos b}, \qquad x_2 = \frac{a \sin b}{\cosh a - \cos b}. \tag{1.3}$$

As shown in Figure 3, the two poles of the bipolar coordinates are located on the x_1 axis at distance $\pm a$, with $a > 0$ (the circles in Figure 1 *a* refers to $a_1 > 0$ and $a_2 < 0$ whereas Fig. 1*b* shows two overlapping circles with $b_1 > 0$ and $b_2 < 0$). Note, that b-coordinate is multi-valued with a discontinuity of 2π across the segment connecting the foci. Hereinafter, we assume $-\pi < b \leq \pi$.

To be specific, we focus on the thermal conductivity problem. Solutions for electric conductivity, diffusion, etc. problems can be obtained by proper renaming of the fields. First, we consider a single inhomogeneity and solve Neumann boundary value problem in two-steps: (1) assessment of the fundamental temperature field related to a remotely applied uniform heat flux in a homogeneous body and (2) fulfilment of the boundary conditions by adding an extra-term to the fundamental field. This solution is used to construct the resistivity contribution tensor of a fiber of interest by calculating proper contour integrals. The resistivity contribution tensor, in turn, is used to calculate overall thermal conductivity of a material containing parallel fibers with the cross-sections shown in Figure 1.

2. Two separate circular holes

We start with the simplest case of two separate holes since it allows the reader to follow the procedure of the solution. Note that a pair of red circles is completely determined by three geometric parameters, for example the radii r_1 and r_2 of two circles and the ligament d between them (Figure 4):

$$x_{c1} = r_1 + d\left[1 - (r_1 + 0.5d)/(r_1 + r_2 + d)\right]; \qquad a_1 = \mathrm{arccosh}\,(x_{c1}/r_1); \qquad a = r_1 \sinh(a_1);$$
$$a_2 = -\,\mathrm{arcsinh}\,(a/r_2); \qquad x_{c2} = -\,r_2 \cosh a_2. \tag{2.1}$$

2.1. Temperature distribution for heat flux in x_1 direction

Let the body be first subjected to a remotely applied steady-state uniform heat flux in x_1 direction, i.e., in bipolar coordinates,

$$\boldsymbol{q}(a,b) = \boldsymbol{q}^{\infty}\left(\frac{1-\cosh a\cos b}{\cosh a-\cos b}, -\frac{\sinh a\sin b}{\cosh a-\cos b}\right) \tag{2.2}$$

The temperature field T is related to the heat flux by Fourier law

$$\boldsymbol{q} = -k\nabla T, \tag{2.3}$$

where k is the thermal conductivity of the body measured in $W/(m\,K)$. Since we are interested in the steady-state solution only, the temperature field T must be harmonic function: $\nabla^2 T = 0$. At the boundary of the inhomogeneity, the Neumann boundary conditions must be satisfied:

$$q_a = 0 \text{ at } a = a_1,\ a = a_2 \tag{2.4}$$

The fundamental temperature field related to a remotely applied uniform heat flux in a homogeneous body can be written

$$T^{\infty}(x_1,x_2) = -\frac{q^{\infty}}{k}x_1;\ \text{i.e.}\quad T^{\infty}(a,b) = -a\frac{q^{\infty}}{k}\frac{\sinh a}{\cosh a-\cos b} \tag{2.5}$$

This field does not satisfy the boundary conditions (2.4). To improve it, we introduce auxiliary harmonic temperature :

$$T^1(a,b) = A + Ba + \sum_{n=1}^{\infty} f_n(a)\cos(nb) \tag{2.6}$$

where

, (2.7)

that produces a corrective heat flux with components

$$\begin{aligned} q_a^1 &= -k\frac{B\cosh a}{a} + k\frac{B\cos b}{a} - k\frac{\cosh a}{a}\sum_{n=1}^{\infty} n\left(C_n e^{na} - D_n e^{-na}\right)\cos nb \\ &\quad + k\frac{\cos b}{a}\sum_{n=1}^{\infty} n\left(C_n e^{na} - D_n e^{-na}\right)\cos nb \\ q_b^1 &= \frac{k}{a}\sum_{n=1}^{\infty} n\left[\cosh a\left(C_n e^{na} - D_n e^{-na}\right) - \cos b\left(C_n e^{na} - D_n e^{-na}\right)\right]\sin nb \end{aligned} \tag{2.8}$$

In particular, component q_a^1 can be expand in Fourier series as

$$\begin{aligned} q_a^1 &= -k\frac{B\cosh a}{a} + k\frac{B\cos b}{a} + \frac{k}{2a}\left(C_1 e^{a} - D_1 e^{-a}\right) + \frac{k}{2a}\sum_{n=1}^{\infty}\left[(n+1)\left(C_{n+1}e^{(n+1)a} - D_{n+1}e^{-(n+1)a}\right)\right. \\ &\quad \left. - 2n\cosh a\left(C_n e^{na} - D_n e^{-na}\right) + (n-1)\left(C_{n-1}e^{(n-1)a} - D_{n+1}e^{-(n+1)a}\right)\right]\cos nb \end{aligned} \tag{2.9}$$

Constants , , C_n and D_n can be obtained from the boundary condition (2.4). For this goal, we use identities (A1) and (A2) given in Appendix that allows one to express component q_a^{∞} of the

remote fluid flow in Fourier series as follows:

$$q_a^{\alpha} = q^{\alpha}\left[e^{-|a|} + \frac{1}{\sinh|a|}\sum_{n=1}^{\infty}\left(2e^{-n|a|} - \cosh a\left(e^{-(n+1)|a|} + e^{-(n-1)|a|}\right)\right)\cos nb\right] \tag{2.10}$$

Since $q_a^{\alpha} + q_a^1 = 0$ for , (with $a_1 > 0$, and $a_2 < 0$), it yields two independent conditions for C_1 and D_1 in the leading terms

$$q^{\alpha} e^{-|a_i|} - \frac{k}{a} B\cosh a_i + \frac{k}{2a}\left(C_1 e^{|a_i|} - D_1 e^{-|a_i|}\right) = 0, \text{ with } i = 1, 2 \tag{2.11}$$

Note, that constant must be equal to zero to avoid violation of the boundary conditions at infinity and constant does not enter the expression for the heat flus and, therefore, can be taken as zero without loss of generality. When the constants and are determined, constants and (with n = 2, 3, é) can be evaluated by imposing $q_a^{\alpha} + q_a^1 = 0$ at the (n- 1)-order terms for $a = a_1$ and . So that

$$C_n = \frac{2aq^{\alpha}}{k}\frac{e^{2na_2} - 1}{e^{2na_1} - e^{2na_2}}, \quad D_n = \frac{2aq^{\alpha}}{k}\frac{e^{2na_2}\left(e^{2na_1} - 1\right)}{e^{2na_1} - e^{2na_2}}, \text{ for } n = 1, 2, \text{ é}. \tag{2.12}$$

2.2. Temperature distribution for heat flux in x_2 direction

We consider now the heat flow in x_2 direction. In bipolar coordinates,

$$\boldsymbol{q}(a,b) = \boldsymbol{q}^{\alpha}\left(\frac{\sinh a\sin b}{\cosh a - \cos b}; -\frac{1 - \cosh a\cos b}{\cosh a - \cos b}\right) \tag{2.13}$$

that corresponds to the following fundamental temperature field in a homogeneous body

$$T^{\alpha}(x_1, x_2) = -\frac{q^{\alpha}}{k}x_2; \text{ i.e. } T^{\alpha}(a,b) = -a\frac{q^{\alpha}}{k}\frac{\sin b}{\cosh a - \cos b} \tag{2.14}$$

Again this temperature field does not satisfy the boundary condition (2.4) and we introduce the auxiliary harmonic temperature field :

$$T^1(a,b) = Ab + Bab + \sum_{n=1}^{\infty} f_n(a)\sin(nb) \tag{2.15}$$

where

, (2.16)

The auxiliary field (2.15) produces a corrective heat flux with components

$$q_a^1 = -k\frac{Bb\cosh a}{a} + k\frac{Bb\cos b}{a} - \frac{k}{a}(\cosh a - \cos b)\sum_{n=1}^{\infty} f_n^{\prime}(a)\sin nb$$

$$q_b^1 = -\frac{k}{a}(\cosh a - \cos b)\left(A + Ba + \sum_{n=1}^{\infty} n f_n(a)\cos nb\right) \tag{2.17}$$

This flux does not affect the remote one since $\boldsymbol{q}^1(a,b) \to 0$ as $a, b \to 0$. Both the remote and corrective heat fluxes can be expanded in Fourier series using expressions (A.3-A.5) in the Appendix. In particular, the a-component of the heat fluxes $\boldsymbol{q}(a,b)$ and $\boldsymbol{q}^1(a,b)$ have the following forms:

$$\begin{aligned} q_a &= -2q \sinh a \sum_{n=1}^{\infty} e^{-n|a|}\sin nb \\ q_a^1 &= -\frac{k}{a}\left[2B\cosh a + \frac{B}{2} + f_1'(a)\cosh a - \frac{1}{2}f_2'(a)\right]\sin b \\ &\quad + \frac{k}{2a}\sum_{n=1}^{\infty}\left[\frac{4B(-1)^n}{n}\left(\cosh a - \frac{n^2}{n^2-1}\right) - 2f_n'(a)\cosh a + f_{n+1}'(a) + f_{n-1}'(a)\right]\sin nb \end{aligned} \tag{2.17}$$

From the boundary condition (2.4) we can write

$$4a\, q e^{-|a_i|}\sinh a_i + k\left[4B\cosh a_i + B + 2f_1'(a_i)\cosh a_i - f_1'(a_i)\right] = 0, \tag{2.18}$$

with $i = 1, 2$; and

$$\begin{aligned} 0 &= 4a\, q e^{-n|a_i|}\sinh a_i \\ &\quad + k\left[\frac{4B(-1)^n}{n}\left(\frac{n^2}{n^2-1} - \cosh a_i\right) + 2f_n'(a_i)\cosh a_i - f_{n+1}'(a_i) - f_{n-1}'(a_i)\right], \quad n = 2, 3, \ldots \end{aligned} \tag{2.19}$$

The first equation provides 2 independent conditions for constants , , C_2, and D_2. Two other conditions can be obtained by multiplying equation (2.19) by $e^{-n|a_i|}$ and summing from n = 2 to infinity:

$$\begin{aligned} &-\frac{2a\, q e^{-2|a_i|}\left(\coth|a_i| - 1\right)\sinh a_i}{k} \\ &+ B\left[2 + \cosh a_i\left(4e^{-|a_i|} - 1 - 8\ln\left(1 + e^{-|a_i|}\right)\right) + \sinh|a_i|\right] - f_1'(a_i)e^{-2a_i} + f_2'(a_i)e^{-a_i} = 0 \end{aligned} \tag{2.20}$$

When constants C_1, D_1, C_2, D_2 have been determined, the remaining constants C_n, D_n can be calculated by imposing condition (2.19) for and at n-order. Constants and are taken as zeros for the same reason as in the previous Section. Finally, after some algebra, we obtain the following expression for constants and :

$$C_n = -\frac{2aq}{k}\frac{e^{2na_2}+1}{e^{2na_1} - e^{2na_2}}, \qquad D_n = -\frac{2aq}{k}\frac{e^{2na_2}\left(e^{2na_1}+1\right)}{e^{2na_1} - e^{2na_2}}, \quad \text{for } n = 1, 2, \ldots. \tag{2.21}$$

Figure 5 shows distribution of the dimensionless temperature $T\ddot{O}\alpha/(r_1 q^{\alpha})$ and normalized heat flux $\boldsymbol{q}/q^{\alpha}$ in a plate subjected to a remote heat flux in x_1 and x_2 directions for $r^{1} r_2/r_1 = 3/5$, $g^{1} d/r_1 = 1$. Figure 6 illustrates the influence of the parameter r on the temperature distribution along the ring of the inhomogeneities keeping fixed the dimensionless ligament g. As shown in this figure, as r increases, temperature decreases in the region between the cavities whereas it increases in the external part of the rings of the holes, i.e. approximately for $0 < q < p/2$. Near highest points of each hole, namely at q @p/2, temperature is almost independent of r. However, temperature variation along the circle $a = a_1$ is smaller than those at $a = a_2$. The effect of the ligament variation (at fixed $r = 2$) is completely different, as shown in Figure 7. In particular, as g increases, the temperature at $a = a_1$ decreases at each point of the contour of the inhomogeneity.

3. Cross-section shape formed by two overlapped circles

The modeling of two overlapping circles differs considerably from the case discussed in Section 2: the circular contours represent two curves of constant b, for a í $(-\alpha, \alpha)$ (Figure 7). In this case, Fourier transforms have to be applied instead of the Fourier series (see, for example, Ling, 1948 and Dutt, 1960). The Neumann boundary conditions at the matrix-inhomogeneity interface have the following form:

$$q_b = 0 \text{ at } b = b_1 > 0 \text{ and} \tag{3.1}$$

while the temperature field T^{α} in the body without inhomogeneity has the form (2.5) that does not satisfy (3.1) and we need to introduce auxiliary (harmonic) temperature fields for heat fluxes in x_1 and x_1 directions.

3.1. Temperature distribution for heat flux in x_1 direction

In this case, we introduce the following auxiliary temperature field

$$T^{1}(a,b) = \int_0^{\alpha} [C_1(s)\cosh sb + C_2(s)\sinh sb]\sin(sa)\, ds \tag{3.2}$$

that produces corrective heat flux with components:

$$q_a^1 = -(\cosh a - \cos b)\frac{k}{a}\int_0^{\alpha} s[C_1(s)\cosh sb + C_2(s)\sinh sb]\cos(sa)\, ds$$

$$q_b^1 = -(\cosh a - \cos b)\frac{k}{a}\int_0^{\alpha} s[C_1(s)\sinh sb + C_2(s)\cosh sb]\sin(sa)\, ds \tag{3.3}$$

Substituting $q_b^1 + q_b^*$ into (3.1) yields

$$s\left[C_1(s)\sinh sb_i + C_2(s)\cosh sb_i\right] = -\frac{2}{p}q^* \sin b_i \frac{a}{k}\int_0^* \frac{\sinh a}{(\cosh a - \cos b_i)^2}\sin(sa)\,da \quad , i = 1, 2. \tag{3.4}$$

Expression (3.4) can be evaluated in closed form using identity (A.6) given in the Appendix ($b_1 > 0$, $b_2 < 0$):

$$C_1(s) = 2q^* \frac{a}{k}\left(\coth ps - 2\frac{\cosh sb_1 \cosh sb_2}{\sinh s(b_1 - b_2)}\right), \; C_2(s) = 2q^* \frac{a}{k}\frac{\sinh s(b_1 + b_2)}{\sinh s(b_1 - b_2)} \tag{3.5}$$

Expressions (3.5) lead to explicit expression for the auxiliary temperature field and, as a result, the total temperature field and the total heat flux field . Note that the corrective heat flux vanishes at , thus preserving the prescribed remote heat flux $\boldsymbol{q}^*$.

Note that corrective temperature field (3.2) can be evaluated in closed form using identity (B3). In particular, at $b = b_1 > 0$ and

$$T^1(a,b) = \frac{aq^*}{2k}\left[\frac{2\sinh a}{(\cosh a) - \cos b_i} + p\frac{\sinh\dfrac{pa}{b_1 - b_2}}{b_1 - b_2}\left(\frac{1}{\cos\dfrac{pb_i}{b_1 - b_2} - \cosh\dfrac{pa}{b_1 - b_2}} - \frac{3}{\cos\dfrac{pb_i}{b_1 - b_2} + \cosh\dfrac{pa}{b_1 - b_2}}\right)\right] \tag{3.5}$$

with *i*, *j* = 1, 2 (*i* ≠ *j*). The first term in expression (3.5) annihilates the remote field (2.5), so that the total temperature coincides with the second term of expression (3.5).

3.2. Temperature distribution for heat flux in x_2 direction

For heat flux in x_2 direction, the auxiliary temperature field has the following form

$$T^1(a,b) = \int_0^* \left[C_1(s)\cosh sb + C_2(s)\sinh sb\right]\cos(sa)\,ds \tag{3.6}$$

It produces corrective heat flux with components:

$$q_a^1 = (\cosh a - \cos b)\frac{k}{a}\int_0^* s\left[C_1(s)\cosh sb + C_2(s)\sinh sb\right]\sin(sa)\,ds$$

$$q_b^1 = -(\cosh a - \cos b)\frac{k}{a}\int_0^* s\left[C_1(s)\sinh sb + C_2(s)\cosh sb\right]\cos(sa)\,ds \tag{3.7}$$

Then, the boundary condition (3.1) for $q_b^1 + q_b^*$ takes the form

$$s\left[C_1(s)\sinh sb_i + C_2(s)\cosh sb_i\right]$$
$$= -\frac{2}{p}q^{\text{¤}}\frac{a}{k}\tilde{\text{ñ}}_0^{\text{¤}}\frac{1-\cosh a\cos b_i}{(\cosh a-\cos b_i)^2}\cos(sa)\,da \quad , i = 1, 2. \tag{3.8}$$

The right hand side of (3.8) can be explicitly evaluated using identities (A.7), (A.8) in the Appendix:

$$C_1(s) = 2q^{\text{¤}}\frac{a}{k}\frac{\sinh s(b_1+b_2)}{\sinh s(b_1-b_2)};\; C_2(s) = -2q^{\text{¤}}\frac{a}{k}\left(\coth ps + 2\frac{\sinh sb_1\sinh sb_2}{\sinh s(b_1-b_2)}\right) \tag{3.9}$$

Using expression (3.9), we can now write explicit expression for the auxiliary temperature field the total temperature field and the total heat flux field . Note that the corrective heat flux vanishes at , similarly to the case considered in section 3.1.

Also in this case, the auxiliary temperature field (25) can be expressed in closed form based on identity (B3) as follows

$$T^1(a,b) = \frac{aq^{\text{¤}}}{k}\left(\frac{\sin b}{\cosh a-\cos b}\right.$$
$$\left.+\frac{p}{b_1-b_2}\left(\frac{\sin\frac{pb}{b_1-b_2}}{\cos\frac{pb_i}{b_1-b_2}-\cosh\frac{pa}{b_1-b_2}}-\frac{\sin\frac{p(b-b_1-b_2)}{b_1-b_2}}{\cos\frac{p(b-b_1-b_2)}{b_1-b_2}+\cosh\frac{pa}{b_1-b_2}}\right)\right) \tag{3.10}$$

with $i, j = 1, 2$ (i Í j). Similarly to the case considered in Section 3.1, the total temperature field $T^1 + T^{\text{¤}}$ coincides with the second term of expression (3.10).

In contrast with the case considered in Section 2, the system of two overlapping circles can be described through different parameters: and , where a is the focal distance and y_{c1} and y_{c2} are vertical coordinates of the centers of the two circles. Figure 9 illustrates the temperature and heat flux distribution around a non-conductive inhomogeneity with the cross-section in the shape of two overlapped circles subjected to a remotely applied heat flow in the x_1 and x_2 directions, for $k_1 = 1/2$ and $k_2 = -1$. Note that, as demanded by boundary conditions, in both cases the heat flux is tangent to the inhomogeneity contour.

The particular case of a lenticular inclusion is illustrated in Figure 10 for $k_1 = -1/2$ and $k_2 = 1$.

4. Lunar cross-section.

In this Section we consider a special case of the overlapped circles when b_1 and b_2 have the same sign. In such a case a cylindrical inclusion has lunar cross-section, as shown in Figure 11. Hereafter,

we assume $b_2 > b_1 > 0$.

4.1. Temperature distribution for heat flux in x_1 direction

Using the axillary temperature field (3.2) and boundary conditions (3.1) for $b_2 > b_1 > 0$ yields the following expressions for $C_1(s)$ and $C_2(s)$

$$C_1(s) = 2q\pi \frac{a}{k} \frac{1}{\sinh s(2p + b_1 - b_2)} \left(\frac{\cosh 2ps \sinh s(p + b_1 - b_2)}{\sinh ps} - \cosh s(b_1 + b_2) \right),$$

$$C_2(s) = 2q\pi \frac{a}{k} \left(\frac{2\cosh sb_1 \sinh sb_2}{\sinh s(2p + b_1 - b_2)} - 1 \right) \tag{4.1}$$

To avoid indefiniteness, the boundary condition (3.1) must be imposed at $2p + b_1$ instead of b_1, as suggested by Liu et al. (1995). Formula (4.1) allows evaluation of the auxiliary temperature field, and after that, the total temperature field and the heat flux.

In some particular cases, a closed form solution can be obtained for the temperature. For example, in the limiting case of arc crack $b_2 - b_1$,

$$T^1(a,b) = \frac{aq\pi}{2k} \left(\frac{\sinh a/2}{\cosh a/2 - \cos b/2} - \frac{\sinh a/2}{\cosh a/2 - \cos(b/2 - b_2)} \right) \tag{4.2}$$

4.2. Temperature distribution for heat flux in x_2 direction

In the case $b_2 > b_1 > 0$, instead of (3.9), we receive the following expressions for $C_1(s)$ and $C_2(s)$

$$C_1(s) = 2q\pi \frac{a}{k} \left(1 + \frac{2\cosh sb_2 \sinh sb_1}{\sinh s(2p + b_1 - b_2)} \right)$$

$$C_1(s) = 2q\pi \frac{a}{k} \left(\frac{\cosh s(p - b_1) \sinh sb_2 - \sinh s(2p + b_1) \cosh s(p - b_2)}{\sinh ps \sinh s(2p + b_1 - b_2)} \right), \tag{4.3}$$

In the limiting case of arc crack, $b_2 - b_1$,

$$T^1(a,b) = \frac{aq\pi}{2k} \left(\frac{\sin b/2}{\cosh a/2 - \cos b/2} - \frac{\sinh(b/2 - b_2)}{\cosh a/2 - \cos(b/2 - b_2)} \right) \tag{4.4}$$

Figure 12 illustrates the distribution of the dimensionless temperature and normalized heat flux around a non-conductive inhomogeneity of lunar shape subjected to a remotely applied heat flow in the x_1 and x_2 directions, for $k_1 = 1$ and $k_2 = 0.5$.

5. Evaluation of the resistivity contribution tensor

Resistivity contribution tensor introduced by Sevostianov and Kachanov (2002) gives the extra temperature gradient produced by introduction of the inhomogeneity into a material subjected to

otherwise uniform heat flux. Following this work, we assume that the isotropic background material of volume V with the thermal conductivity k_0 contains an isolated inhomogeneity of volume V_1 of the isotropic thermal conductivity k_1. The limiting cases $k_1 = 0$ and $k_1 = \infty$ correspond to a non-conductive and a superconducting inhomogeneities; the present work focuses on a non-conductive inhomogeneity. Assuming linear relation between temperature gradient ∇T and the heat flux vector $\boldsymbol{q}$ per reference volume (Fourier law) for both the constituents, the change in ∇T required to maintain the same heat flux after the inhomogeneity is introduced is given by

$$\Delta(\nabla T) = \frac{V_1}{V} \boldsymbol{R} \cdot \boldsymbol{q}, \tag{5.1}$$

where the symmetric second-rank tensor $\boldsymbol{R}$ is called the *resistivity contribution tensor* of the inhomogeneity.

For a non-conductive inhomogeneity, the additional temperature gradient due to its presence can be represented as integral over the inhomogeneity boundary

$$\Delta(\nabla T) = \frac{1}{V} \int_{\partial W} T \boldsymbol{n} \, dS, \tag{5.2}$$

where T and $\boldsymbol{n}$ are temperature and outward unit vector normal to the boundary, respectively. Thus, Neumann boundary value problem for Laplace equation has to be solved in order to find the resistivity contribution tensor of a non-conductive inhomogeneity. In the case of an infinite fiber, the component along the fiber axis (let it be x_3 axis) is independent of the shape of the cross-section (see, for example, Torquato, 2002) and can be calculated separately as

$$\frac{A_1}{A} R_{33} = \frac{1}{q_3^0} \Delta(\nabla T) \cdot \boldsymbol{e}_3 = \frac{A_1}{A} (k_1 - k_0) \tag{5.3}$$

where A_1 is the area of the cross-section occupied by the inhomogeneity, is the area of the cross-section of the reference volume normal to the axis of the fiber, and q_3^0 is the magnitude of the remote heat flus along x_3 axis. For non-conductive inhomogeneity, $k_1 = 0$, and $R_{33} = -k_0$. If the principal axes of the inhomogeneity are not known, the other components of the resistivity contribution tensor are (see Radi and Sevostianov, 2016)

$$\begin{pmatrix} R_{11} \\ R_{21} \end{pmatrix} = \frac{1}{q_1^0 A_1} \int_{\partial W} T_1(a,b) \begin{pmatrix} n_1 \\ n_2 \end{pmatrix} ds; \quad \begin{pmatrix} R_{12} \\ R_{22} \end{pmatrix} = \frac{1}{q_2^0 A_1} \int_{\partial W} T_2(a,b) \begin{pmatrix} n_1 \\ n_2 \end{pmatrix} ds \tag{5.4}$$

where, q_1^0 and q_2^0 are the magnitudes of the remotely applied heat fluxes along x_1 and x_2 axes, respectively, and $T_1(a,b)$ and $T_2(a,b)$ are the related total temperature fields (calculated in Sections 2-5). The contour integral is performed around the boundary of the inhomogeneity cross-section ∂W of the inhomogeneity, $\boldsymbol{n} = n_1 \boldsymbol{e}_1 + n_2 \boldsymbol{e}_2$ is the outward unit vector normal to the contour

of the inhomogeneity, and ds is the infinitesimal arc length.

5.1. Two separate circular inhomogeneities (symmetric with respect to x_1 axis)

The components of the unit vector and the infinitesimal arc length on the contour of the two circles with $a = const$ are:

$$n_1 = \frac{\cosh a_i \cos b - 1}{\cosh a_i - \cos b} sign(a_1),\ n_2 = \frac{\sinh|a_i| \sin b}{\cosh a_i - \cos b}$$

$$ds = r_i dq = \frac{a\ sign(a_i)}{\cosh a_i - \cos b} db, \qquad i = 1, 2 \tag{5.5}$$

where q is the polar angle measured from x_1 axis as reported in Figure 3. Then, using results of the Section 2 and formulas (A.16)-(A.17) in the Appendix, expression (5.4) with $A_i = p r_i^2$ ($i = 1, 2$) yields the components of the resistivity contribution tensor R_{ij} (i, j = 1, 2) in the following form ($a_1 > 0, a_2 < 0$):

$$R_{11} = \frac{1}{k}\left\{-1 + \frac{2k}{aq^{\text{¤}}\left(\text{csch}^2 a_1 + \text{csch}^2 a_2\right)} \ddot{a}_{n=1}^{\text{¤}} n\left[e^{-na_1} f_n(a_1) - e^{-na_2} f_n(a_2)\right]\right\}$$

$$R_{22} = \frac{1}{k}\left\{-1 + \frac{2k}{aq^{\text{¤}}\left(\text{csch}^2 a_1 + \text{csch}^2 a_2\right)} \ddot{a}_{n=1}^{\text{¤}} n\left[e^{-na_1} f_n(a_1) + e^{-na_2} f_n(a_2)\right]\right\} \tag{5.6}$$

and . Note that terms $-1/k$ in eqns (5.6) represent the contribution of the remote temperature fields $T^{\text{¤}}$. The remaining terms are due to the auxiliary solution T^1. Figure 13 illustrates dependence of the normalized components of the resistivity contribution tensor (5.6) on at different values of .

5.2. Overlapped circles symmetric with respect to x_2 axis.

The component of the unit vector and the infinitesimal arc length on the contour at $b = const$ are

$$n_1 = \frac{\sinh a \sin b_i}{\cosh a - \cos b_i} sign(b_1),\ n_2 = \frac{1 - \cosh a \cos b}{\cosh a - \cos b_i} sign(b_i)$$

$$ds = r_i dq = -\frac{a\ sign(b_i)}{\cosh a - \cos b_i} da, \qquad i = 1, 2 \tag{5.7}$$

Taking into account that $A_i = r_i^2\left(p - \left|b_i + \left(\sin|2b_1|\right)/2\right|\right)$, $i = 1, 2$ and using (5.4) and results of Section3, one can write

$$R_{11} = \frac{2a^2 p}{Ak(b_1 - b_2)}\left\{\frac{ki}{\sin kb_1}\sum_{m=1}\left[L_m(b_1) - (-1)^m L_m(b_2)\right]\sin kmb_1 + \frac{ki}{\sin kb_2}\sum_{m=1}\left[L_m(b_2) - (-1)^m L_m(b_1)\right]\sin kmb_2\right\}$$

$$R_{22} = \frac{4a^2 p}{Ak(b_1 - b_2)}\left\{\sum_{m=1}\left[S_m(b_1) + (-1)^m S_m(b_2)\right]\sin kmb_1 + \frac{ki}{\sin kb_2}\sum_{m=1}\left[S_m(b_2) + (-1)^m S_m(b_1)\right]\sin kmb_2\right\} \qquad (5.8)$$

where

$$A = A_1 + A_2,\ k = p/(b_1 - b_2)$$

$$L_m(b) = (m-1)\left[F\left(e^{-ib},1,k(m-1)\right) - F\left(e^{ib},1,k(m-1)\right)\right] - (m+1)\left[F\left(e^{-ib},1,k(m+1)\right) - F\left(e^{ib},1,k(m-1)\right)\right]$$

$$S_m(b) = 1 + km\left[e^{-ib}F\left(e^{-ib},1,km\right) + e^{ib}F\left(e^{ib},1,km\right)\right]$$

and $F(z,s,a) \equiv \sum_{k=0}\frac{z^k}{(a+k)^s}$ is Lerch function.

The geometry of the cross-section is completely determined by two dimensionless parameters : and . Particular case of $k_1 < 0$ and $k_2 > 0$ describes a lenticular inhomogeneity, and the limit $k_1 \to -\infty$, $k_2 \to \infty$ (i. e. $b_1 \to p$, $b_2 \to -p$) corresponds to a rectilinear crack of length $2a$ along x_1 axis with opening $x \to 0$. In this case (5.8) is reduced to

$$R_{11} = 0; \qquad R_{22} = \frac{1}{xk} \to \infty \qquad (5.9)$$

The contribution of the rectilinear crack into the overall resistivity, however, is finite:

$$\frac{A_1}{A}R_{22} = \frac{1}{A}\frac{pa^2}{k} \qquad (5.10)$$

(is the area of the cross-section of the reference volume normal to the axis of the fiber). This result coincides with one given by Zimmerman (1996)

The case $k_1 = k_2 = 0$ corresponds to an isolated circular inhomogeneity. In this case, the well known result is covered

$$R_{11} = R_{22} = 2/k \qquad (5.11)$$

A semicircular inhomogeneity is described by $k_1 \to 0$, $k_2 \to \infty$. Expressions (5.8) are also valid for an inhomogeneity of lunar shape when $k_1 > k_2$ and $A_* = A_1 - A_2$. Figures 14 and 15 illustrate dependence of the normalized components of the resistivity contribution tensor (5.8) on

at different values of . In the limiting case of a circular arc crack (k_1 - k_2) results coincide with ones of Sevostianov (2006):

$$\frac{A_1}{A}R_{11} = \frac{1}{A}\frac{p}{2k}R^2(1-\cos a)(3+\cos a)$$
$$\frac{A_1}{A}R_{22} = \frac{1}{A}\frac{p}{2k}R^2(1-\cos a)^2 \qquad (5.12)$$

In the case of *multiple* fibers, one can start with the non-interaction approximation when each inhomogeneity is subject to the same far-field heat flux, unperturbed by the presence of the surrounding fibers. In this case, the contribution of each fiber into the effective resistivity of the material can be treated separately and the effective conductivity tensor $\boldsymbol{K}_{eff}$ is expressed in terms of a sum $\frac{1}{V}\sum_i V_i \boldsymbol{R}^{(i)}$ over individual inhomogeneities:

$$k_0\boldsymbol{K}_{eff} = \left[\boldsymbol{I} + \frac{k_0}{V}\sum_i V_i \boldsymbol{R}^{(i)}\right]^{-1} \qquad (5.13)$$

The non-interaction approximation is of fundamental importance: besides being reasonably accurate at small concentrations of inhomogeneities (up to 15-20% for fiber reinforced composites, Sevostianov and Sabina, 2008), it constitutes the basic building block for various homogenization schemes that place non-interacting inhomogeneities into a certain effective matrix or effective field. Detailed description of the connection between various homogenization schemes and non-interaction approximation is given, for example, in the review of Sevostianov and Kachanov (2013).

6. Concluding remarks.

We solved analytically the problem on distribution of temperature field and heat flux around a non-conductive cylindrical inhomogeneity, having a cross-section formed by two separate or overlapping circles, embedded in an isotropic material subjected to a steady heat flux at infinity. The solution is obtained in the form of infinite series which rapidly converge. Four types of cross-sections are considered (Figure 1): (a) two separate circles (auxiliary problem), (b) cross-section formed by union of two overlapping circles of generally different radii, (c) lenticular cross-section (that is mathematically a particular case of two overlapping circles), and (d) lunar cross-section (including arc crack as a limiting case). The obtained solution is used to construct resistivity contribution tensor for non-conductive inhomogeneities of the considered shape ï the quantity that describes extra temperature gradient due to the presence of the inhomogeneity. The limiting cases of a fiber of circular cross-section, rectilinear crack, and arc crack are recovered.

The resistivity contribution tensor is the key quantity for calculation of the effective properties of the material. The obtained results can be reformulated for the electric conductivity and

diffusion process (in the electric conductivity problem, temperature and heat flux should be replaced by electric potential and electric current; in the diffusion problem they should be replaced by concentration and diffusion flux).

Note, the reciprocity theorem of Keller (1964) as and Schulgasser (1992) can be used to obtain the effective conductivity of an isotropic material containing superconductive inhomogeneities from the solution for a material with the same microstructure and non-conductive inhomogeneities. Indeed, as follows from formula (1) in Schulgasser (1992) paper

$$k_{eff}\left(k_0, \text{ø}k_0\right)k_{eff}\left(k_0, k_0/\text{ø}\right) = k_0^2 \qquad (6.1)$$

where the first argument in k_{eff} represents conductivity of the matrix k_0 and the second ï conductivity of the inhomogeneities. As $\text{ø} \to 0$, one can get the connection between effective properties of the materials containing non-conductive and superconductve inhomogeneities.

Unfortunately, this approach cannot be used directly to construct resistivity contribution tensor for an inhomogeneity of finite conductivity: it is possible for elliptical shapes only (Zimmerman, 1989, 1996; Chen et al, 2017). In this case, the boundary value problem with non-zero boundary conditions at the matrix/inhomogeneity interface has to be solved. This problem is much more difficult than the one discussed in the present paper.

Acknowledgement.

Financial support from NASA Cooperative Agreement NNX15AL51H to New Mexico State University (IS) and from the Italian Ministry of Education, University and Research (MIUR) in the framework of the Project Project PRIN ``COAN 5.50.16.01" (code 2015JW9NJT) are gratefully acknowledged.

References

Dutt, S.B. (1960) On the stresses due to an overlapped circular hole on the neutral axis of a deep beam under constant bending moment. *Applied Scientific Research,* **9**,457-462

Ekneligoda, T.C. and Zimmerman, R.W. (2006) Compressibility of two-dimensional pores having n-fold axes of symmetry. *Proc. R. Soc. A*, **462**, 1933ï1947.

Ekneligoda, T.C. and Zimmerman, R.W. (2008b) Boundary perturbation solution for nearly-circular holes and rigid inclusions in an infinite elastic medium. *ASME J. Appl. Mech.*, **75**, paper 011015-1.

Ekneligoda, T.C. and Zimmerman, R.W. (2008a) Shear compliance of two-dimensional pores possessing N-fold axis of rotational symmetry. *Proc. R. Soc. A*, **464,** 759ï775.

Givoli, D. and Elishakoff, I. (1992) Stress concentration at a nearly circular hole with uncertain

irregularities, *J. Appl. Mech*, **59**(2S), S65-S71.

Jasiuk, I. (1995) Cavities vis-a`-vis rigid inclusions: elastic moduli of materials with polygonal inclusions. *International Journal of Solids and Structures* **32**, 407ï422.

Jeffery, G. B. (1921). Plane stress and plane strain in bipolar co-ordinates. Philos. Trans. R. Soc. London, Ser. A, 221, 265-293.

Kachanov, M., Tsukrov,I., Shafiro,B. (1994). Effective moduli of solids with cavities of various shapes. *Appl. Mech. Rev.*, **47**, S151-S174.

Ling C-B (1948) The Stresses in a Plate Containing an overlapped circular hole. *J. Appl. Phys*., **19**, 405-411

Liu, Y., Tang, B., Gao, Y., (1995) Electric Field Penetration and Perturbation Problems of a Nonuniform Cylindrical Cavity with a Slot. *IEEE Transactions on Electromagnetic Compatibility*, **37**, 458-462.

Liu, W., Huang, C., and Jin, X. (2015) Electrospinning of grooved polystyrene fibers: effect of solvent systems. *Nanoscale Research Letters*, **10**, 237

Marcuzzo J.S., Otani, C., Polidoro, H.A., and Otani, S. (2013) Influence of thermal treatment on porosity formation on carbon fiber from textile PAN. *Materials Research*, **16**, 137-144

Monteiro, S.N., Satyanarayana, K.G., Ferreira, A.S., Nascimento, D.C.O., Lopes, F.P.D., Silva, I.L.A. , Bevitori, A.B., Inácio, W.P., Bravo Neto, J., and Portela, T.G. (2011) Selection of high strength natural fibers. *Revista Matéria*, **15**, 488 ï 505,

Radi E, Sevostianov I., (2016) Toroidal insulating inhomogeneity in an infinite space and related problems, Proceedings of the Royal Society A, 472, 20150781.

Sevostianov, I. (2006) Thermal conductivity of a material containing cracks of arbitrary shape *International Journal of Engineering Sciences*, **44**, 513-528.

Sevostianov, I. and Kachanov, M. (2002) Explicit cross-property correlations for anisotropic two-phase composite materials. *Journal of the Mechanics and Physics of Solids*, **50**, 253-282.

Sevostianov, I. and Kachanov, M. Non-interaction approximation in the problem of effective properties. Chapter 1 in: *Effective Properties of Heterogeneous Materials* (M. Kachanov and I. Sevostianov, Eds), Springer, 2013, 1-96.

Torquato, S. (2002). *Random Heterogeneous Materials: Microstructure and Macroscopic Properties.* Springer.

Tsukrov, I., Novak, J. (2002) Effective elastic properties f solids with defects of irregular shape. *Int. J. Solids Struct*., **39**, 1539-1555.

Tsukrov, I., Novak, J. (2004) Effective elastic properties of solids with two-dimensional inclusions of irregular shape. *Int. J. Solids Struct*., **41**, 6905-6924.

Zimmerman, R.W. (1986) Compressibility of two-dimensional cavities of various shapes. *J. Appl.*

Mech., **53**, 500-504.

Zimmerman, R.W. (1996) Effective conductivity of a two-dimensional medium containing elliptical inhomogeneities, *Proc. Roy. Soc. Lond.* **A453**, 1713-1727.

Appendix A. Auxiliary formulas.

1. Identities involving trigonometric and hyperbolic functions.

$$\frac{1}{\cosh a - \cos b} = \frac{1}{\sinh|a|} + \frac{2}{\sinh|a|}\sum_{n=1}^{\infty} e^{-n|a|}\cos nb, \qquad -\pi \le b \le \pi \tag{A.1}$$

$$\frac{\cos b}{\cosh a - \cos b} = \coth|a| - 1 + \frac{1}{\sinh|a|}\sum_{n=1}^{\infty}\left(e^{-(n+1)|a|} + e^{-(n-1)|a|}\right)\cos nb, \quad -\pi \le b \le \pi \tag{A.2}$$

$$\frac{\sin b}{\cosh a - \cos b} = 2\sum_{n=1}^{\infty} e^{-n|a|}\sin nb \tag{A.3}$$

$$b = -2\sum_{n=1}^{\infty}\frac{(-1)^n}{n}\sin nb \tag{A.4}$$

$$b\cos b = -\frac{1}{2}\sin b + 2\sum_{n=2}^{\infty} n\left(\frac{(-1)^n}{n^2 - 1}\right)\sin nb \tag{A.5}$$

2. Fourier transforms used in Section 3

$$\int_0^{\infty}\frac{\sinh a\,\sin(sa)}{(\cosh a - \cos b)^2}\,da = s\pi\,\frac{\sinh s\pi\cosh sb - \cosh s\pi\sin|sb|}{\sinh s\pi\sin|b|} \tag{A.6}$$

$$\int_0^{\infty}\frac{\cos(sa)}{(\cosh a - \cos b)^2}\,da = \pi\,\frac{\cosh sb\left(s\coth s\pi + \cot|b|\right) - \sinh sb\left(s + \cot|b|\coth s\pi\right)}{\sin^2 b}; \tag{A.7}$$

$$\int_0^{\infty}\frac{\cosh a\,\cos(sa)}{(\cosh a - \cos b)^2}\,da = \pi\,\frac{s\cosh s(\pi - |b|)\cot|b| + \csc^2 b\sinh s(\pi - |b|)}{\sinh s\pi\,\sin^2|b|}; \tag{A.8}$$

$$\int_0^{\infty}\frac{\cos(sa)}{\cosh a - \cos b}\,da = \pi\,\frac{\cosh sb\sinh s\pi - \sinh|sb|\cosh s\pi}{\sinh s\pi\sin|b|}; \tag{A.9}$$

$$\int_0^{\infty}\frac{\cosh a\cos(sa)}{\cosh a - \cos b}\,da = \pi\,\frac{\sinh s(\pi - |b|)\cos b}{\sinh s\pi\sin|b|}; \tag{A.10}$$

$$\int_0^{\infty}\frac{1}{\cosh a - \cos b}\,da = \frac{\pi - |b|}{\sin|b|}; \tag{A.11}$$

$$\int_0^{\infty}\frac{1}{(\cosh a - \cos b)^3}\,da = \pi\,\frac{3\cot|b| + (\pi - |b|)(3\csc^2 b - 2)}{2\sin^3|b|}; \tag{A.12}$$

$$\int_0^{\infty}\frac{\sinh^2 a}{(\cosh a - \cos b)^3}\,da = \frac{\pi - |b| + \sin|b|\cos b}{2\sin^3|b|}; \tag{A.13}$$

$$\int_0^{\infty} \frac{\cosh bs \quad \sin sa}{\sinh cs}\, ds = \frac{\pi}{2|c|} \frac{\sinh \frac{\pi a}{c}}{\cos \frac{\pi b}{c} + \cosh \frac{\pi a}{c}} \tag{A.14}$$

3. Definite integrals used for evaluation of resistivity contribution tensors

$$\int_{-\pi}^{\pi} \frac{\cos nb}{\cosh a - \cos b}\, db = \frac{2\pi}{\sinh|a|} e^{-|na|}; \tag{A.15}$$

$$\int_{-\pi}^{\pi} \frac{\cos nb}{(\cosh a - \cos b)^2}\, db = \frac{2\pi}{\sinh^2 a} e^{-|na|}\left(n + \coth|a|\right) \tag{A.16}$$

$$\int_{-\pi}^{\pi} \frac{\cos nb}{(\cosh a - \cos b)^3}\, db = \frac{2\pi}{\sinh^3|a|} e^{-|na|}\left(\frac{n^2}{2} + n^2 + 3n\coth|a| + \frac{3}{\sinh^{2a}}\right) \tag{A.17}$$

$$\int_{-\pi}^{\pi} \frac{b\sin b}{\cosh a - \cos b}\, db = 4\pi \ln\left(1 + e^{-|a|}\right); \tag{A.18}$$

$$\int_{-\pi}^{\pi} \frac{b\sin b}{(\cosh a - \cos b)^2}\, db = \frac{4\pi}{\left(1 + e^{|a|}\right)\sinh|a|} \tag{A.19}$$

$$\int_{-\pi}^{\pi} \frac{\sin^2 b}{(\cosh a - \cos b)^3}\, db = \frac{\pi}{\sinh^3|a|} \tag{A.20}$$

4. Identities involving Lerch function.

$$F(z, s, a) \equiv \sum_{k=0}^{\infty} \frac{z^k}{(a+k)^s} \tag{A.21}$$

For $k > 0$ and $k \neq b$

$$\begin{aligned} &\int_0^{\infty} \frac{\sin a \sin ka}{(\cosh ka - \cos b_2)(\cosh a - \cos b_1)^2}\, da \\ &= \frac{k\,i}{\sin b_1 \sin kb_2} \sum_{m=1}^{\infty} \left\{(m-1)\left[F\left(e^{-ib_1}, 1, k(m-1)\right) - F\left(e^{ib_1}, 1, k(m-1)\right)\right]\right. \\ &\left. - (m+1)\left[F\left(e^{-ib_1}, 1, k(m+1)\right) + F\left(e^{ib_1}, 1, k(m+1)\right)\right]\right\} \sin kmb_2 \end{aligned} \tag{A.22}$$

$$\begin{aligned} &\int_0^{\infty} \frac{\sinh a \sinh ka}{(\cosh ka + \cos b_2)(\cosh a - \cos b_1)^2}\, da \\ &= \frac{k\,i}{\sin b_1 \sin kb_2} \sum_{m=1}^{\infty} (-1)^m \left\{(m-1)\left[F\left(e^{-ib_1}, 1, k(m-1)\right) - F\left(e^{ib_1}, 1, k(m-1)\right)\right]\right. \\ &\left. - (m+1)\left[F\left(e^{-ib_1}, 1, k(m+1)\right) + F\left(e^{ib_1}, 1, k(m+1)\right)\right]\right\} \sin kmb_2 \end{aligned} \tag{A.23}$$

$$\int_0^{\infty} \frac{1-\cosh a\cos b}{(\cosh a-\cos b_1)^2} e^{-ka}\,da = 1+k\left[e^{-ib}F\left(e^{-ib},1,1+k\right)+e^{ib}F\left(e^{ib},1,1+k\right)\right] \qquad \text{(A.24)}$$

Figure captions

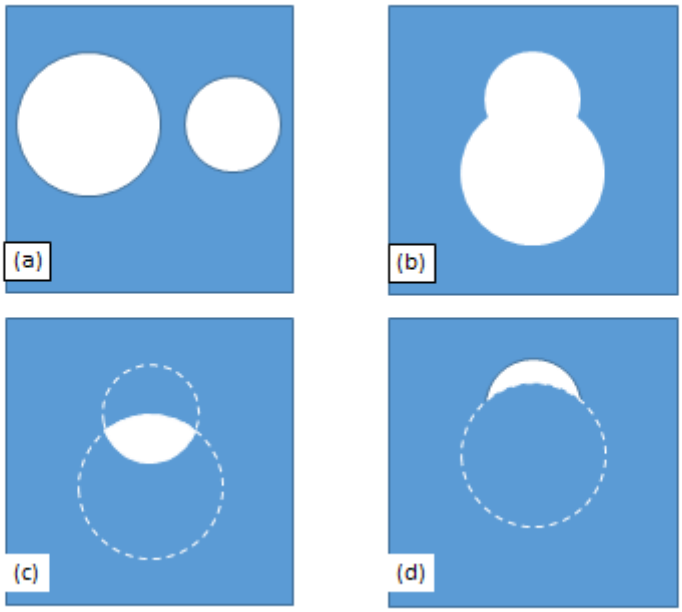

Figure 1

Figure 1. (a) two separate circles (auxiliary problem), (b) cross-section formed by union of two overlapping circles of generally different radii, (c) lenticular cross-section (that is mathematically a particular case of two overlapping circles), and (d) lunar cross-section (including arc crack as a limiting case).

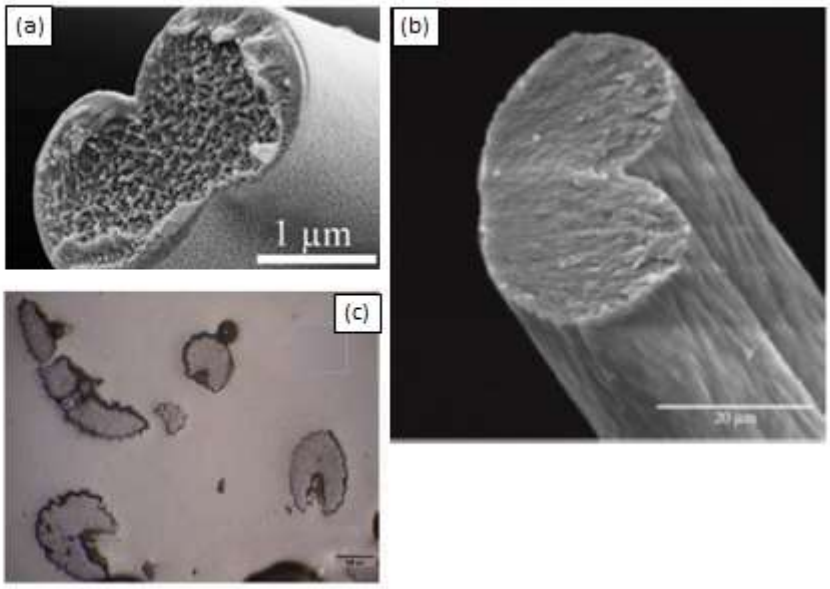

Figure 2

Figure 2. Examples of the fibers with cross-sections formed by two circles occurring in natural and man-made materials: (a) electrospinned polystyrene fiber (from Liu et al, 2015) (b) oxidized polyacrylonitrile fiber (from Marcuzzo et al, 2013) (c) natural sisal fiber (Monteiro et al, 2011).

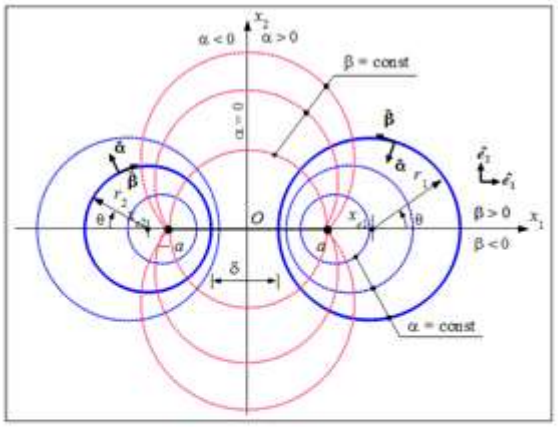

Figure3

Figure 3. Sketch of the bipolar coordinate system.

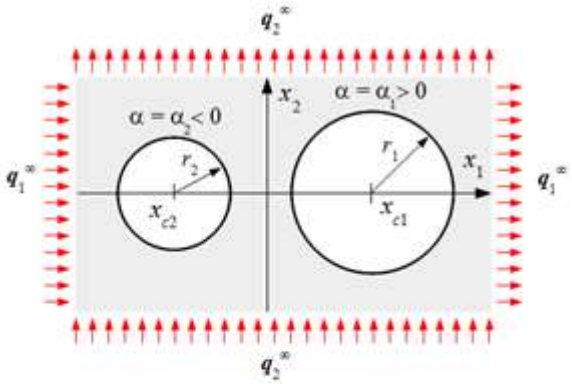

Figure4

Figure 4. Sketch of an infinite plate with two separate circular inhomogeneities.

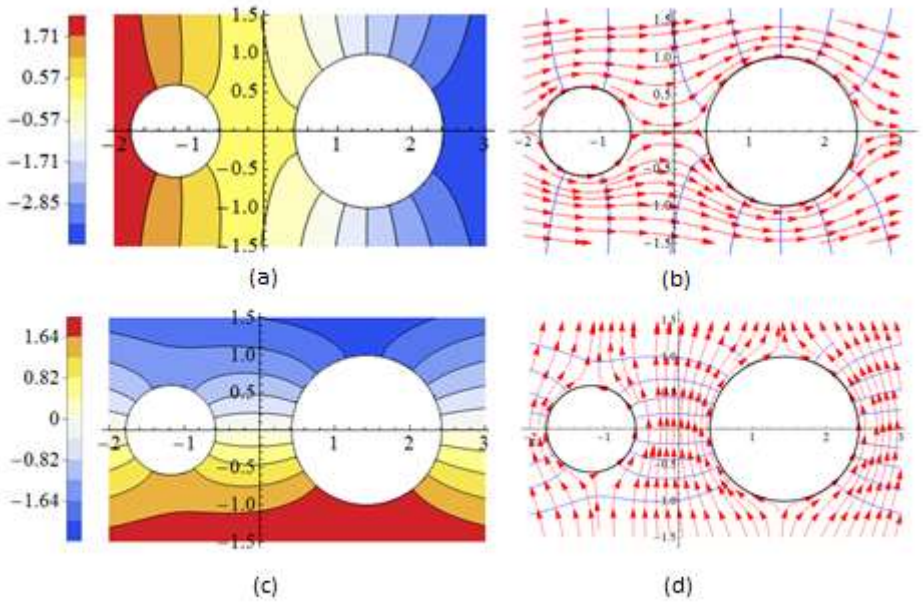

Figure5

Figure 5. Distribution of the dimensionless temperature ((a) and (c)) and dimensionless heat flow ((b) and (d)) in a plate subjected to a remote heat flux in the x_1 ((a) and (b)) and x_2 ((c) and (d)) directions for $r = 3/5$, $g = 1$.

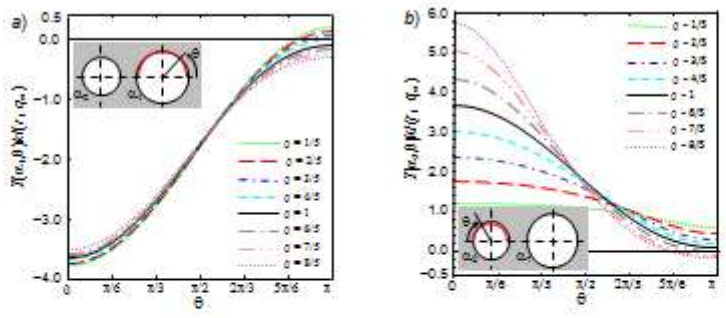

Figure6

Figure 6. Dimensionless temperature $T(a,b)\ k/(r_1\ q^{\infty})$ along the contour of the hole (a) with $a = a_1$ and (b) with $a = a_2$ for some values of r and $g = 1$.

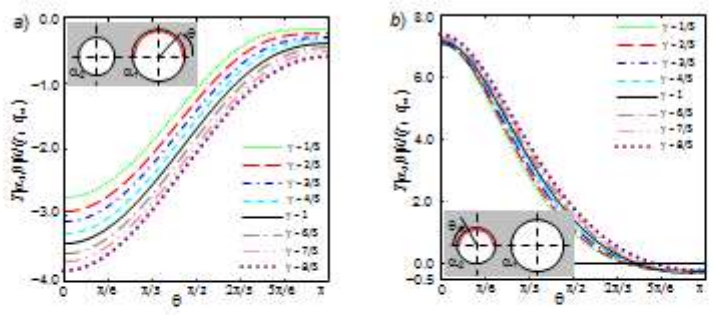

Figure7

Figure 7. Dimensionless temperature $T(a,b)\ k/(r_1\ q^{\infty})$ along the contour of the hole (a) with $a = a_1$ and (b) with $a = a_2$ for some values of g and $r = 2$.

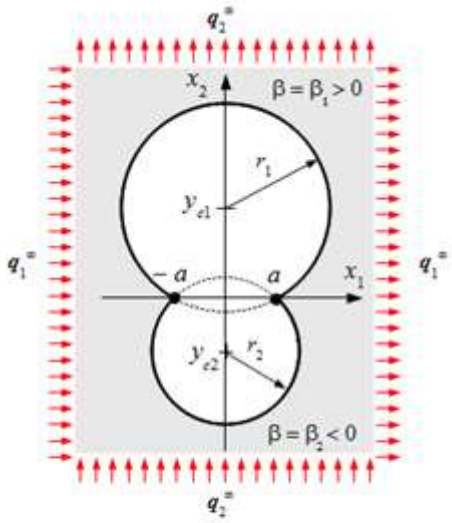

Figure8

Figure 8. Sketch of an infinite plate with two merging holes subjected to a remote heat flow along the principal directions x_1, x_2.

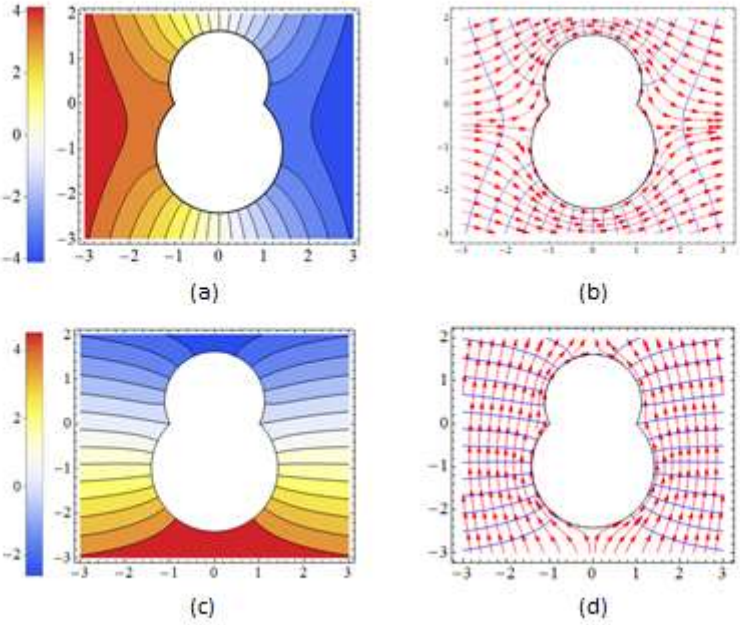

Figure9

Figure 9. Distribution of the dimensionless temperature ((a) and (c)) and heat flow ((b) and (d)) in a plate subjected to a remote heat flux in the x_1 ((a) and (b)) and x_2 ((c) and (d)) directions for $k_1 = 1/2$ and $k_2 = -1$.

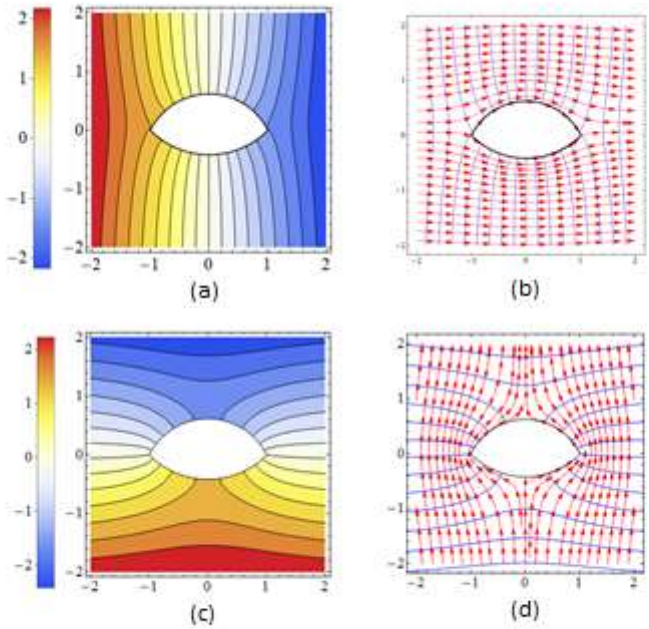

Figure10

Figure 10. Distribution of the dimensionless temperature ((a) and (c)) and heat flow ((b) and (d)) in a plate subjected to a remote heat flux in the x_1 ((a) and (b)) and x_2 ((c) and (d)) directions for $k_1 = -1/2$ and $k_2 = 1$.

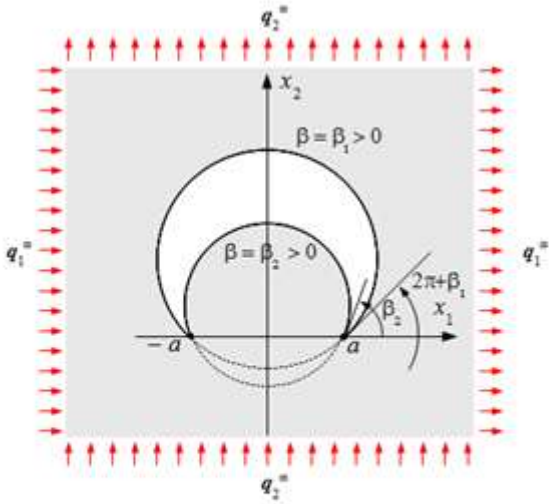

Figure11

Figure 11. Lunar shaped inclusion. Note that the domain is described starting from the internal circle ($b = b_2$), so that quantities on the outer circle ($b = b_1$) must be evaluated at $b = 2p + b_1$.

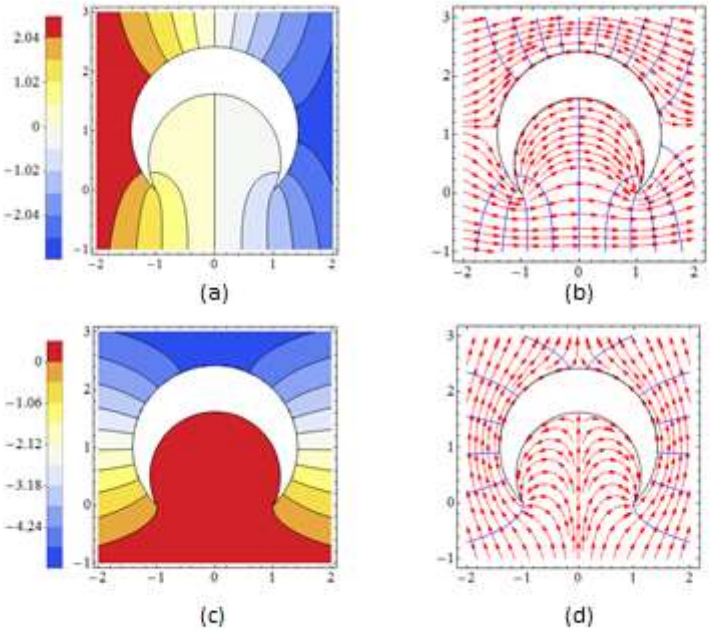

Figure12

Figure 12. Distribution of the dimensionless temperature ((a) and (c)) and heat flow ((b) and (d)) in a plate subjected to a remote heat flux in the x_1 ((a) and (b)) and x_2 ((c) and (d)) directions for $k_1 = 1$ and $k_2 = 1/2$.

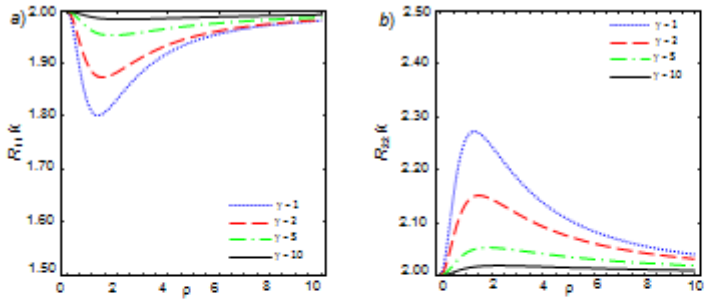

Figure13

Figure 13. Dimensionless components of the resistivity contribution tensor: (*a*) R_{11} *k* and (*b*) R_{22} *k* for g = 1, 2, 5, 10 varying r .

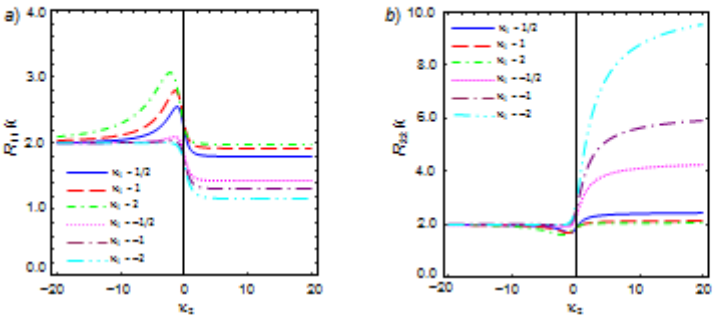

Figure14

Figure 14. Dimensionless components of the resistivity contribution tensor for overlapping inclusions: *a*) R_{11} *k* and *b*) R_{22} *k* for k_1 = ° 1/2, ° 1, ° 2, varying k_2. Dashed lines concern lenticular inclusions.

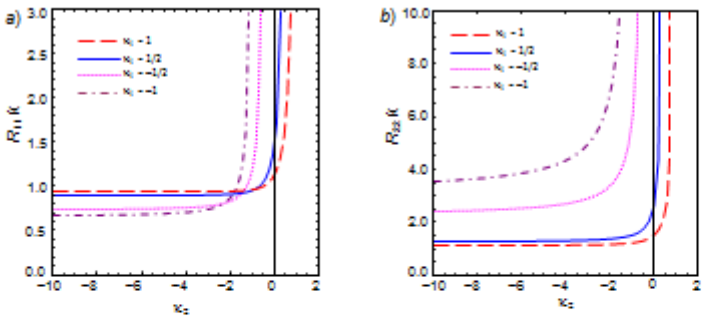

Figure 15

Figure 15. Dimensionless components of the resistivity contribution tensor for lunar inclusions: *a*) $R_{11}\,k$ and *b*) $R_{22}\,k$ for $k_1 = ° 1/2, ° 1, ° 2$, varying k_2..